Maria Helena Braga, Luis Filipe Malheiros, Fernando Castro, and Delfim Soares**
GMM/IMAT, DEMET, FEUP, Porto, Portugal; *Universidade do Minho, Guimarães, Portugal

Experimental Liquidus Points and Invariant Reactions in the Cu–Zr System

In the Cu–Zr system, especially between $0.25 < x(Zr) < 1$, experimental liquidus points are missing and many doubts arise concerning the invariant points. In 1986, Kneller et al. [1] pointed out the existence of three phases and two eutectoid reactions which had not yet been reported. This work has been questioned by other authors [2, 3]. Differential Thermal Analysis (DTA) experiments have been done in almost the whole range of compositions of the Cu–Zr system, especially where the work of Kneller et al. [1] is ambiguous; results are compared with the previous ones.

1 Introduction

The phase diagram of the Cu–Zr system was firstly and essentially based on the work of Lundin et al. [4]. In their work thermal analysis was used to determine eutectic and peritectic isotherms as well as compound melting points. Metallographic examination was used to reveal the phases present at the equilibrium. Lundin et al. [4] reported the existence of five eutectics at the concentrations/temperatures $x(Zr) = 0.065$ / 1283 K, $x(Zr) = 0.382$ / 1160 K, $x(Zr) = 0.440$ / 1163 K, $x(Zr) = 0.540$ / 1200 K, $x(Zr) = 0.724$ / 1268 K, four congruently melting intermetallic phases with stoichiometries/melting temperatures Cu_3Zr / 1373 K, Cu_3Zr_2 / 1168 K, CuZr / 1208 K, $CuZr_2$ / 1273 K and one phase that is formed peritectically at 1343 K.

In subsequent works, two more phases were reported, Cu_9Zr_2 [5] and Cu_5Zr [6 to 9]. Further, it was pointed out that the compositions of some of the phases are different from those originally proposed and should be corrected, $Cu_3Zr \rightarrow Cu_{51}Zr_{14}$ [10], $Cu_5Zr_2 \rightarrow Cu_8Zr_3$ [11], $Cu_3Zr_2 \rightarrow Cu_{10}Zr_7$ [12].

Structures were reported for the phases Cu_5Zr [13], $Cu_{51}Zr_{14}$ [10], Cu_8Zr_3 [11, 14], $Cu_{10}Zr_7$ [12] (the authors made intensity calculations with the positional parameters for $Ni_{10}Zr_7$ from [15]), CuZr [16] and $CuZr_2$ [17].

Moreover, it has been shown by Carvalho and Harris [16] that the B2-type phase, CuZr, is stable only above 985 ± 5 K; below this temperature, it decomposes by an eutectoid reaction into the neighbouring phases, presumably $Cu_{10}Zr_7$ and $CuZr_2$. These authors also concluded from magnetic susceptibility measurements, metallography and X-ray diffraction evidence that, at rapid cooling from the stability range, CuZr transforms martensitically into a metastable phase with unknown structure; the transformation temperature is 440 ± 5 K. They stated that a clear X-ray diffraction pattern of the equilibrium phase CuZr was not obtained by annealing stoichiometric alloy samples just below the melting point and subsequent quenching, but only in a sample quenched from the liquid state.

Kneller et al. [1] studied the system in the range $0.20 \le x(Zr) \le 0.70$, reported the existence of three new phases and gave their X-ray data, $Cu_{24}Zr_{13}$, $CuZr_{1+z}(z \cong 3)$, Cu_5Zr_8, and a superstructure of $CuZr_2$. Phase stabilities were established for temperatures above 800 K. They reported that all new intermetallic phases in this system have equal sphere packing densities and their lattice parameters are commensurable, i. e. connected by simple geometrical ratios. As a consequence of such universal geometrical compatibility, structural coherency may play an important role in phase reactions. Further, they concluded that the DTA measurements indicate at least two high-temperature phases, one at $x(Zr) \cong 0.33$, tentatively termed Cu_2Zr, and one at $x(Zr) \cong 0.35$, tentatively termed $Cu_{24}Zr_{13}$. None of these phases could be retained at room temperature by annealing and subsequent quenching. Nevertheless, alloys with $0.36 \le x(Zr) \le 0.38$, quenched from the melt, yielded the clear X-ray pattern of a new phase which was ascribed to $Cu_{24}Zr_{13}$. They found the work of Carvalho and Harris [16] for the structure and stability range of the phase CuZr compatible with their results. However, they measured the lattice stability to be slightly higher and concluded that CuZr appears to be formed by a peritectic reaction rather than having a congruent melting temperature, according to their DTA curves, and that its composition seemed to be not exactly $x(Zr) = 0.50$ but somewhat higher, $x(Zr) \cong 0.515$. Kneller et al. [1] also proposed the existence of two more eutectoid reactions $Cu_8Zr_3 \leftrightarrow Cu_{51}Zr_{14} + Cu_{10}Zr_7$ (at 885 K) and $Cu_5Zr_8 \leftrightarrow Cu_{10}Zr_7 + CuZr_2$ (below $\sim$ 970 K) and for $CuZr_2$ a low-temperature phase modification, $CuZr_2$-L, and a high temperature modification, $CuZr_2$-H, stable above $\sim$ 1200 K.

The Cu–Zr system has already been assessed by several authors [2, 3] and [18]. Zeng et al. [3] considered the existence of the phases Cu_5Zr, $Cu_{51}Zr_{14}$, Cu_8Zr_3, $Cu_{10}Zr_7$, CuZr and $CuZr_2$ but omitted, as Arias and Abriata [2], the new phases and eutectoid reactions observed by Kneller et al. [1]. In their opinion, the existence of these new phases should be confirmed independently by other authors. On the other hand, they questioned the experimental procedures used by Kneller et al. [1].

Braga et al. [18] assessed the Cu–Zr system taking into account the work of Kneller et al. [1]. The present work aims to clear some doubts still remaining.

Table 1. DTA experimental points.

Concentration x(Zr)	Temperature (K)	Heating Rate (K/min)
0.800	1124	5
0.800	1240	5
0.800	1300	5
0.785	1240	10
0.785	1286	2
0.663	1198	2
0.663	1204	2
0.663	1234	2
0.663	1299	*
0.652	1192	10
0.652	1194	10
0.652	1221	10
0.652	1279	5
0.640	1191	2
0.640	1195	2
0.640	1224	2
0.640	1282	2
0.608	1005	10
0.608	1186	5
0.608	1188	5
0.608	1219	5
0.608	1265	5
0.600	1186	2
0.600	1188	2
0.600	1218	2
0.600	1257	*
0.581	1006	10
0.581	1189	5
0.581	1219	5
0.581	1243	5
0.573	1005	10
0.573	1185	5
0.573	1186	5
0.573	1209	5
0.573	1234	5
0.550	1184	2
0.550	1215	2
0.550	1229	2
0.543	1177	2.5
0.543	1181	2.5
0.543	1202	2.5
0.543	1220	2.5
0.537	999	10
0.537	1193	2
0.537	1196	2
0.537	1228	2
0.537	1242	*
0.515	1006	10
0.515	1187	2
0.515	1190	2
0.515	1224	2
0.515	1239	2
0.500	1171	10
0.500	1183	10
0.500	1195	10
0.500	1233	2
0.485	1169	5
0.485	1182	5
0.485	1218	5
0.470	1174	10
0.470	1186	10
0.470	1206	10
0.439	999	10
0.439	1172	2
0.439	1204	2
0.406	1194	2
0.406	1197	2
0.406	1198	2
0.406	1202	*
0.395	1195	2
0.395	1200	*
0.376	1196	2
0.376	1201	2
0.376	1233	*
0.360	1191	2
0.360	1195	2
0.360	1229	2
0.360	1238	2
0.360	1272	2
0.339	1196	2
0.339	1232	2
0.339	1241	2
0.339	1273	2
0.339	1310	*
0.335	1203	10
0.335	1241	10
0.335	1251	10
0.335	1277	10
0.335	1313	10
0.303	1187	5
0.303	1218	5
0.303	1262	5
0.303	1299	5
0.303	1341	5
0.300	1187	5
0.300	1218	5
0.300	1262	5
0.300	1299	5
0.300	1351	5
0.286	1184	2
0.286	1219	2
0.286	1269	2
0.286	1296	2
0.286	1367	*
0.259	1275	5
0.259	1304	5
0.259	1385	5
0.246	1270	5
0.246	1306	5
0.246	1382	5
0.231	1270	10
0.231	1306	10
0.231	1376	10
0.153	1270	10
0.153	1309	10
0.153	1359	10
0.139	1266	10
0.139	1313	10
0.139	1331	10
0.128	1275	10
0.128	1311	10
0.128	1320	10
0.106	1272	10
0.100	1273	10
0.100	1287	10
0.060	1271	10
0.060	1310	10

* These points were extrapolated for a heating rate equal to "zero".

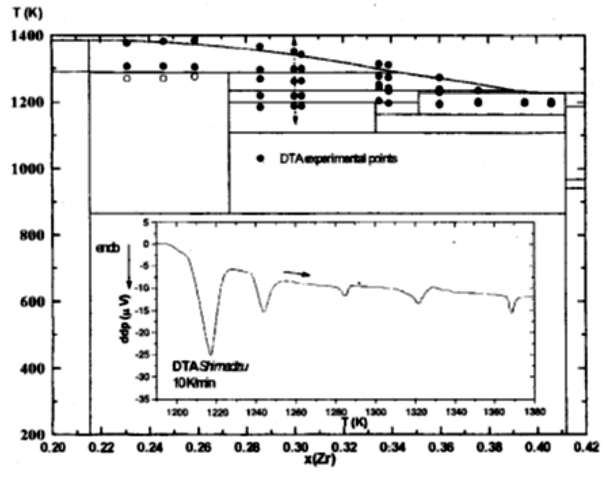

Fig. 1. Assessed phase diagram [18]; DTA experimental points. DTA curve (first heating) for a composition corresponding to the dotted arrow. The open circles are the experimental points, obtained for the samples annealed for 96 h at 1103 K.

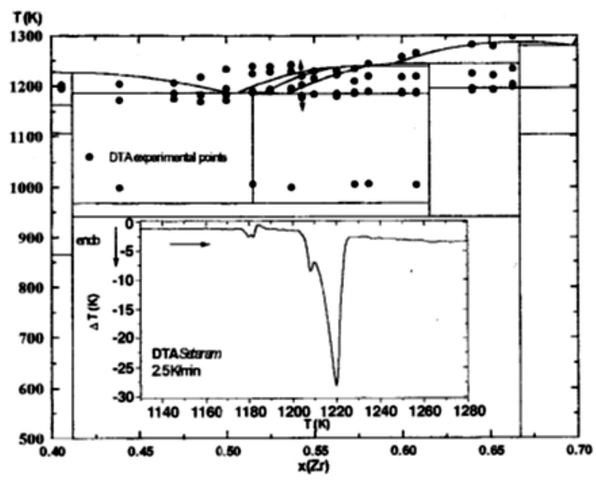

Fig. 2. Assessed phase diagram [18]; DTA experimental points. DTA curve for a composition corresponding to the dotted arrow.

2 Experimental

For each composition to be investigated, a master alloy of 1 g or 2 g was prepared from pure elements, 99.99 wt.% Cu and 99.9 wt.% Zr, by melting in an arc furnace under a purified argon atmosphere; prior to the introduction of the argon, primary vacuum was made in the chamber of the furnace. Each alloy was homogenised by remelting.

Some of the samples were annealed at 1103 K for 24 h under vacuum and the samples with compositions $0.215 < x(\mathrm{Zr}) < 0.273$ were annealed at the same temperature for 24 h and 96 h under a purified argon atmosphere.

Some focus was put on the compositions that might solve some questions, so, the most scanned range of concentrations was $0.22 < x(\mathrm{Zr}) < 0.67$.

The chemical composition of the master alloys was determined in an X-ray fluorescence spectrometer X-UNIC II, with an average accuracy of 5.6 %. Some samples were analysed by energy-dispersive spectroscopy (EDS).

DTA (differential thermal analysis) measurements took place in three different apparatus, DTA Shimadzu, DTA/TGA Setaram, DTA/TGA TA Instruments SDT 2960 (all three from room temperature to 1773 K) under a purified argon atmosphere.

The DTA measurements were carried out in Al_2O_3 crucibles. SEM (scanning electron microscopy) – EDS (energy-dispersive spectroscopy) measurements were made to ensure that the samples did not react with the crucibles.

For each concentration, the heating was performed at least four times with four different samples with heating rates of 2 K/min, 5 K/min, 10 K/min and 20 K/min. For some compositions two cycles of heating/cooling were done. The reactivity of copper and zirconium with oxygen, at high temperatures, did not allow us to consider, mainly for samples rich in Cu, the DTA curve for a heating rate of 2 K/min.

Liquidus points were extrapolated to a heating rate of "0 K/min", when possible, with the values for at least

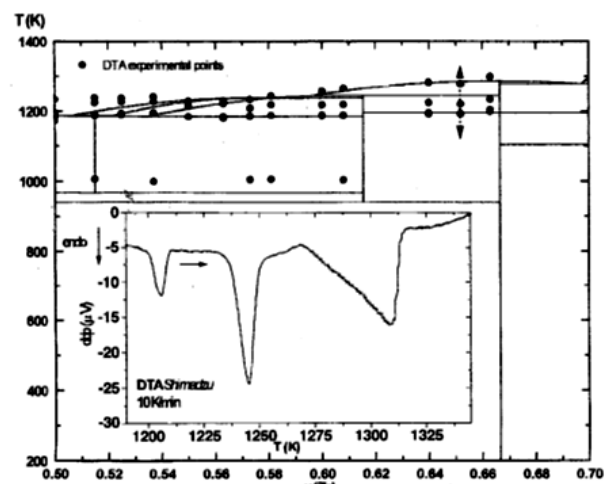

Fig. 3. Assessed phase diagram [18]; DTA experimental points. DTA curve for a composition corresponding to the dotted arrow.

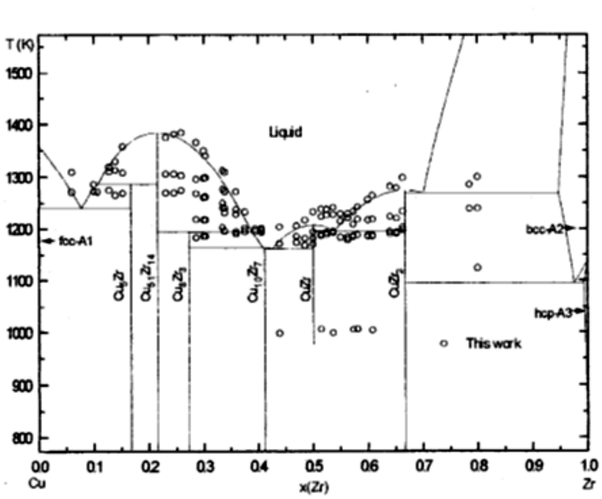

Fig. 4. Comparison between Zeng et al. [3] assessed phase diagram (taken from COST 507 database [19] for Thermo Calc [20]) and the experimental points of this work.

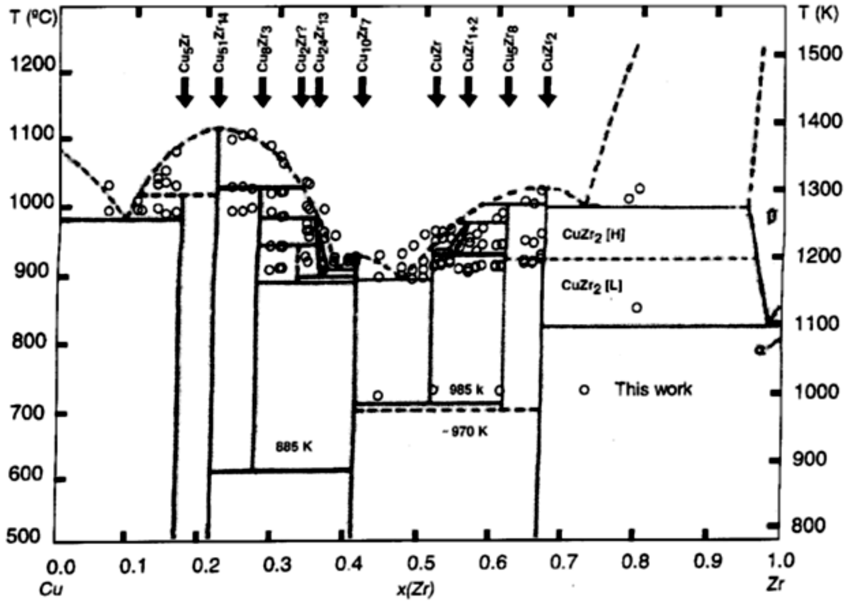

Fig. 5. Comparison between Kneller et al. [1] assessed phase diagram and the experimental points of this work (superimposed to the phase diagram scanned from Kneller et al. [1]).

the heating rates of 2 K/min, 5 K/min, 10 K/min and 20 K/min. The invariant temperatures were taken from the 2 K/min curve (when it was possible).

The accuracy is ± 5 K and sometimes higher for lower temperatures.

3 Phase Diagram

DTA results are presented in Table 1.

Comparisons were made between the DTA values obtained in this work, the published assessed phase diagrams [1, 3, 18] (Figs 1 to 5) and the published experimental points (Fig. 6).

Figures 1, 2 and 3 show the DTA heating curves for compositions where there are doubts concerning the phase diagram.

4 Conclusions

1. None of the phase diagrams already published is totally coherent with the experimental DTA points obtained in this work.
2. For compositions $0 < x(\mathrm{Zr}) < 0.2$, the assessed phase diagram which is closer to the experimental points, here presented, is the one from Kneller et al. [1]. The reactions L $\leftrightarrow$ fcc-Al + Cu_5Zr and L + $Cu_{51}Zr_{14}$ $\leftrightarrow$ Cu_5Zr have in [1] (Fig. 5) more accurate temperature and composition values. Nevertheless, the liquidus curve L / L + $Cu_{51}Zr_{14}$ is in agreement with experimental points in the three works [1, 3, 18]. It should be emphasised that, to prevent the oxidation of the Cu, these points were taken from experimental curves obtained with a heating rate of 10 K/min.

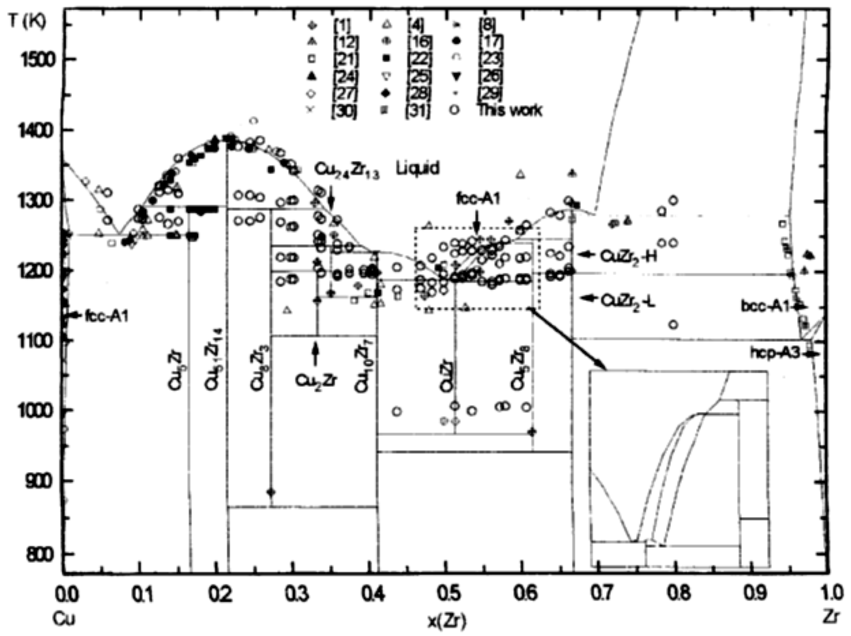

Fig. 6. Comparison between Braga et al. [18] assessed phase diagram and all the experimental points already available.

3. For compositions $0.2 < x(Zr) < 0.45$ the assessment of Kneller et al. [1] is still the closest one, although in our experiments the temperature of the peritectic decomposition of Cu_8Zr_3 seems to be lower than in [1], when considering the experimental points for samples with compositions $x(Zr) = 0.231$, $x(Zr) = 0.246$ and $x(Zr) = 0.259$. The DTA measurements were performed with these samples, after being annealed for 24 h and 96 h at 1103 K (samples with ~ 150mg weight) under a purified argon atmosphere. The experiments made with the samples annealed during 96 h still reveal the existence of the points represented by open circles in the phase diagram of Fig. 1. These points can only be confirmed by X-ray diffraction at high temperatures.
4. From the analysis of DTA experiments, for compositions of $0.273 \leq x(Zr) \leq 0.335$, it can be inferred that at least another phase is stable between ~ 1190 K and ~ 1300 K. This phase could be $Cu_{24}Zr_{13}$ or/and Cu_2Zr as suggested by Kneller et al. [1].
5. In the range $0.47 \leq x(Zr) \leq 0.55$ the liquidus curve is very different from other works [1, 3, 18]. The shape of the curve seems to indicate the presence of a phase, with congruent melting, for $x(Zr) \cong 0.50$.
6. For compositions $0.55 < x(Zr) \leq 0.67$ the experimental liquidus curve is too different from the one from Kneller et al. [1] but very similar to those in [3] and [18].
7. Taking into account the peaks for samples with compositions $0.439 \leq x(Zr) \leq 0.667$, $x(Zr) = 0.785$ and $x(Zr) = 0.800$, it can be inferred that the transformation $CuZr_2$-L $\leftrightarrow$ $CuZr_2$-H occurs at ~ 1230 K and not at 1200 K.
8. The peak corresponding to the eutectoid reaction $Cu_8Zr_3 \leftrightarrow Cu_{51}Zr_{14} + Cu_{10}Zr_7$ at 885 K could not be observed. However, SEM/EDS measurements, after DTA measurements, in samples with compositions $0.231 \leq x(Zr) \leq 0.335$, showed the existence of the phases $Cu_{51}Zr_{14}$ and $Cu_{10}Zr_7$ indicating that the reaction occurred.
9. A peak at ~ 523 K was observed for samples with compositions $0.439 \leq x(Zr) \leq 0.667$ that could correspond, as it was proposed by Carvalho and Harris [16], to the CuZr martensitic transformation into a metastable phase of unknown structure.
10. At ~ 1000 K a peak occurs in the DTA curves of the samples with compositions $0.55 < x(Zr) \leq 0.67$, that could be interpreted as the reaction $CuZr \leftrightarrow Cu_{10}Zr_7 + CuZr_2 - L$. No evidences of a second peak were detected. Thus, the existence of the reaction $Cu_5Zr_8 \leftrightarrow Cu_{10}Zr_7 + CuZr_2$-L is not confirmed.

To clear away some doubts left concerning the phases present in the phase diagram the authors are currently studying the system using SEM/EDS and X-ray diffraction.

The authors would like to thank the Portuguese Science Program PRAXIS XXI for the PhD bourse (BD / 3349 / 94). The authors would like to thank Prof. José Domingos Santos for his contributions to this work. The contribution of Mr. José Soares from CINFU in the metallographic preparation of the samples is also acknowledged.

Literature

1. *Kneller, E.; Khan, Y.; Gorres, U.:* Z. Metallkd. *77* (1986) 43–48.
2. *Arias, D.; Abriata, J.P.:* Bull. Alloy Phase Diagrams *11* (1990) 452–459.
3. *Zeng, K.-J.; Hämäläinen, M.; Lukas, H.L.:* J. Phase Equilibria *15* (1994) 577–586.
4. *Lundin, C.E.; McPherson, D.J.; Hansen, M.:* Trans. AIME *197* (1953) 273–278.
5. *Vitek, J.M.:* Z. Metallkd. *67* (1976) 559–563.
6. *von Hillmann, G.; Hofmann, W.:* Z. Metallkd. *56* (1956) 279–286.
7. *Petrescu, M.:* Bull. Inst. Polytechnic "Georghe GheorghiuDej", Bucaresti, Seria Chimie-Metalurgie *39* (1977) 79.
8. *Perry, A.J.; Hugi, W.:* J. Inst. Met. *100* (1972) 378–380.
9. *Karlson, N.:* J. Inst. Met. *79* (1951) 391.
10. *Gabathuler, J.P.; White, P.; Parthé, E.:* Acta Cryst. B *31* (1975) 608–610.
11. *Bsenko, L.:* J. Less-Common Met. *40* (1975) 365–366.
12. *Glimois, J.L.; Forey, P.; Feron, J.L.:* J. Less-Common Met. *113* (1985) 213–224.
13. *Forey, P.; Glimois, J.L.; Feron, J.L.:* J. Less-Common Met. *124* (1986) 21–27.
14. *Bsenko, L.:* Acta Cryst. B *32* (1976) 2220–2224.
15. *Kirkpatrick, M.E.; Smith, J.F.; Larsen, W.L.:* Acta Cryst. *15* (1962) 894–903.
16. *Carvalho, E.M.; Harris, I.R.:* J. Mater. Sci. *15* (1980) 1224–1230.
17. *Augustson, R.N.:* U. S. Atomic Energy Commission Publ., AECD-3456 (1950) 3–46.
18. *Braga, M.H.; Ansara, I.; Malheiros, L.F.:* Proceedings of CALPHAD XXV, Erice-Italy, 26 to 31 May, 1996.
19. COST-507, Thermochemical Database for Light Metal Alloys Concerted Action on Materials Sciences, in: I. Ansara (ed.), European Commission DGXII Publ., (1994) 132–134.
20. *Sundman, B.; Jasson, B.; Andersson, J.O.:* CALPHAD *9* (1985) 153–190.
21. *Allibone, T.E.; Sykes, C.:* J. Inst. Met. *39* (1928) 173–189.
22. *Pogodin, S.A.; Shumova, I.S.; Kugucheva, F.A.:* Dokl. Akad. Nauk SSSR *27* (1940) 670–672.
23. *Raub, E.; Engel, M.:* Z. Metallkd. *39* (1948) 172–177.
24. *Douglass, D.L.; Morgan R.E.:* Trans. Metall. Soc. AIME *215* (1959) 869–870.
25. *Saarivirta, M.J.:* Trans. Metall. Soc. AIME *218* (1960) 431–437.
26. *Showak, W.:* Trans. Metall. Soc. AIME *224* (1962) 1297–1298.
27. *Zwicker, U.:* Metal. *16* (1962) 409–412.
28. *Donachie Jr., M.J.:* J. Inst. Met. *92* (1964) 180.
29. *Kawakatsu, I.; Suzuki, H.; Kitano, H.:* J. Japan. Inst. Met. *31* (1967) 1253–1257.
30. *Korol'kov, A.M.; Lysova, E.L.:* Struktura i Svoistva Legk. Splavov, Nauka, Moscow (1971) 17–20.
31. *Kuznetsov, G.M.; Fedorov, V.N.; Rodnyanskaya, A.L.; Nikonova, A.V.:* Sov. Non-Ferrous Met. Res. *6* (1978) 267–268.

(Received February 19th, 1998)

Correspondence Addresses

M.H. Braga, L.F. Malheiros
GMM/IMAT, DEMET, FEUP
Rua dos Bragas
4099 Porto Codex, Portugal

F. Castro, D. Soares
Dep. Eng. Mecânica da Universidade do Minho
Campus de Azurém
4800 Guimarães, Portugal